

In Vitro and in Vivo Trypanosomicidal Activity of Pyrazole-Containing Macrocyclic and Macrobicyclic Polyamines: Their Action on Acute and Chronic Phases of Chagas Disease

Manuel Sánchez-Moreno,^{*,†} Clotilde Marín,[†] Pilar Navarro,^{*,‡} Laurent Lamarque,[‡] Enrique García-España,^{*,§} Carlos Miranda,[‡] Oscar Huertas,[†] Francisco Olmo,[†] Fernando Gómez-Contreras,^{||} Javier Pitarch,[§] and Francisco Arrebola[⊥]

[†] Departamento de Parasitología, Facultad de Ciencias, and [⊥] Departamento de Histología, Facultad de Medicina, Universidad de Granada, E-18071 Granada, Spain

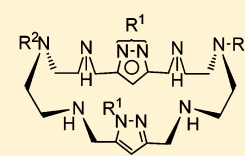
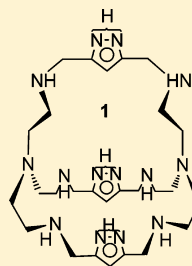
[‡] Instituto de Química Médica, Centro de Química Orgánica M. Lora-Tamayo, CSIC, E-28006 Madrid, Spain

[§] Departamento de Química Inorgánica, Instituto de Ciencia Molecular, Universidad de Valencia, E-46980 Paterna (Valencia), Spain

^{||} Departamento de Química Orgánica, Facultad de Química, Universidad Complutense, E-28040 Madrid, Spain

S Supporting Information

ABSTRACT: The in vitro and in vivo anti-*Trypanosoma cruzi* activity of the pyrazole-containing macrobicyclic polyamine **1** and *N*-methyl- and *N*-benzyl-substituted monocyclic polyamines **2** and **3** was studied. Activity against both the acute and chronic phases of Chagas disease was considered. The compounds were more active against the parasite and less toxic against Vero cells than the reference drug benznidazole, but **1** and **2** were especially effective, where cryptand **1** was the most active, particularly in the chronic phase. The activity results found for these compounds were complemented and discussed by considering their inhibitory effect on the iron superoxide dismutase enzyme of the parasite, the nature of the metabolites excreted after treatment, and the ultrastructural alterations produced. A complementary histopathological analysis confirmed that the compounds tested were significantly less toxic to mammals than the reference drug and that **1** and **2** exhibited lower levels of damage than **3**.



- 2**, R¹=Me; R²=H
3, R¹= Bn; R²=H
4, R¹=H; R²=(CH₂)₇Me

INTRODUCTION

Chagas disease (trypanosomiasis) is a potentially fatal parasitic disease that is recognized by the World Health Organization (WHO) as being one of the world's most neglected tropical diseases. It is widespread throughout Latin America¹ and is caused by a protozoan, *Trypanosoma cruzi*, which is primarily transmitted by some species of blood-feeding triatomine insects, mainly *Triatoma infestans*, *Rhodius prolixus*, and *Triatoma dimidiata*.² This disease can also be transmitted by nonvectorial mechanisms, including blood transfusion or organ donation,³ transfer from mother to child during pregnancy,⁴ or even the ingestion of food contaminated by the parasite.⁵ Because of increasing international travel and immigration, this disease has spread not only across all of Latin America, but across the United States, Canada, Spain, Italy, and other countries.^{6,7} The best estimates of Chagas disease cases in Latin America report 10–14 million infected people. The initial, acute infection is usually asymptomatic, where most patients do not realize that they have been contaminated with the parasite; this is because the parasite load is fairly small.⁸ The acute phase can further evolve into a chronic stage, in which about 30% of infected individuals develop severe cardiac, peripheral nervous system, or digestive complications, sometimes within 10–30

years after infection, and many of them will suffer cardiac failure and sudden death.⁹ The control and treatment of Chagas disease constitutes a very large economic burden for Latin American countries.

The main drugs currently used to treat Chagas disease are two nitroaromatic heterocycles: the furane-based nifurtimox and the imidazole-based benznidazole (BZN).¹⁰ Both drugs are effective in the acute phase of the disease, although benznidazole shows a better safety and efficacy profile,¹¹ but the efficacy of both is very low in the chronic phase.¹² Furthermore, these compounds have severe side effects, including anorexia, vomiting, peripheral polyneuropathy, and allergic dermatopathy. The presence of nitro groups attached to the heterocyclic rings suggests that these drugs act on the parasite by nitro reduction, originating reduced intermediates that covalently modify biomolecules, although its mode of action is currently under discussion.¹³ Their high level of toxicity against humans is probably a result of oxidative or reductive tissue damage and is inextricably linked to their

Received: December 20, 2011

Published: March 26, 2012

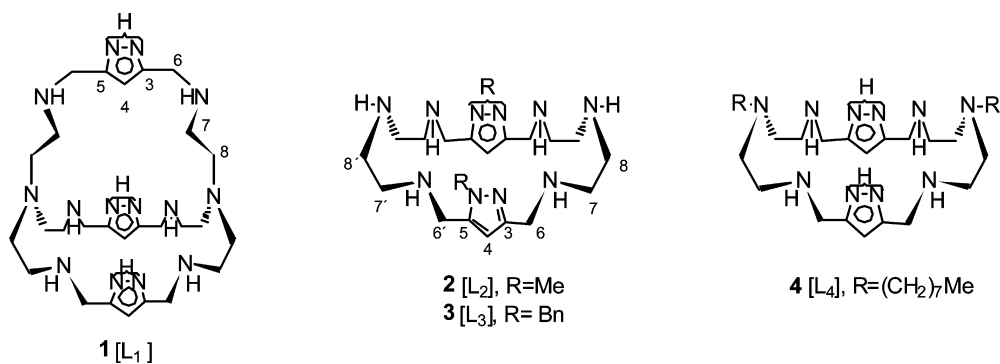
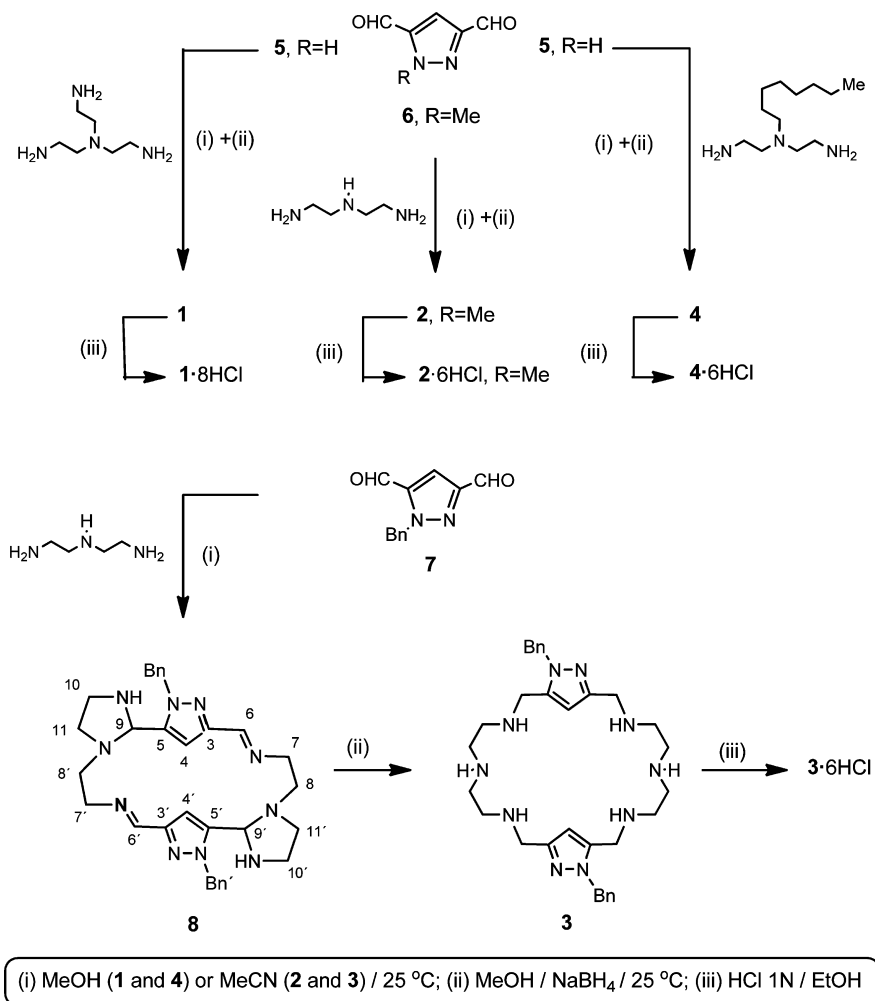


Figure 1. Macrocyclic and macrobicyclic pyrazole-containing polyamines tested in this work.

Scheme 1. Preparation of the Pyrazole-Based Macrocycles



antiparasitic activity.¹⁰ Therefore, less toxic and more selective drugs are urgently needed.⁶

One promising target for new drugs against Chagas disease is iron superoxide dismutase (Fe-SOD). It has been shown that parasitic protozoan survival is closely related to the ability of some enzymes to evade toxic free-radical damage.¹⁴ One of the main protective mechanisms involves Fe-SOD, a specific enzyme of trypanosomatids that acts as a scavenger of superoxide ions and hydroxyl radicals.¹⁵ Since prosthetic groups are essential in all enzymatic processes, modifications in the enzyme active site of Fe-SOD by dissociation of the

metal ion or by changes in the coordination geometry could be effective ways to deactivate its antioxidant features, and they would presumably affect both the growth and survival of parasite cells. Closely connected to this idea, in previous work our research group synthesized 1,4-bis(alkylamino)benzo[*g*]-phthalazine derivatives capable of forming dinuclear complexes with transition metals; so far we have shown that, in the free form, they are selective inhibitors of Fe-SOD and that they simultaneously show remarkable *in vitro* and *in vivo* activity against *T. cruzi*.^{16,17} We proposed that one feasible mechanism

Table 1. In Vitro Activity, Toxicity, and Selectivity Index for Compounds 1-4 against Extra- and Intracellular Forms of *T. cruzi*^a

	IC ₅₀ (μM)			Vero cells ^c	SI ^d		
	epimastigote forms ^b	axenic amastigote forms ^b	intracellular amastigote forms ^b		epimastigote forms	axenic amastigote forms	intracellular amastigote forms
BZN	15.9 ± 1.1	18.9 ± 1.5	23.3 ± 4.6	13.6 ± 0.9	0.8	0.7	0.6
1	1.3 ± 0.1	7.2 ± 2.2	6.2 ± 0.8	149.1 ± 13.5	114.7 (143)	20.7 (30)	24.0 (40)
2	1.3 ± 0.3	8.8 ± 1.8	6.5 ± 1.6	178.5 ± 21.3	137.3 (172)	20.3 (29)	27.5 (46)
3	16.5 ± 3.2	10.0 ± 2.9	13.8 ± 2.5	195.4 ± 11.7	11.8 (15)	19.5 (28)	14.2 (24)
4	46.4 ± 7.4	20.8 ± 3.5	18.4 ± 3.3	21.5 ± 3.3	0.5 (0.6)	1.0 (1.4)	1.1 (1.8)

^aThe results are averages of three separate determinations. ^bIC₅₀ = the concentration required to give 50% inhibition, calculated by linear regression analysis from the K_c values at the concentrations used (1, 10, 25, 50, and 100 μM). ^cAfter 72 h of culture. ^dSelectivity index = IC₅₀ Vero cells toxicity/IC₅₀ activity of extracellular or intracellular forms of the parasite. In parentheses are: the number of times that the compound SI exceeded the reference drug SI.

for their trypanosomicidal activity could be related to competition for the metal ion of Fe-SOD.¹⁷

The promising results obtained from the open-chain ligands mentioned above prompted us to focus our attention on the series of macrocyclic compounds 1–4 (Figure 1). We had previously proposed a macrobicyclic polyamine containing three 3,5-disubstituted pyrazole rings with the structure 1,^{18,19} and two monocyclic dinuclear polyamines endowed with N-Me²⁰ (2) or N-Bn²¹ (3) substituted pyrazole rings have also been described. Now we have synthesized these three polyamines with a higher grade of purity in both the free and hydrochloride forms, which, in the case of 2, required the design of improved synthesis and purification procedures. In addition, a more lipophilic pyrazole-containing dinuclear polyamine with bulky octyl groups attached to the amine nitrogens at the side chains (4), which had also been described previously, was prepared again.²² These compounds were selected because it is well-known that polyaminic macrocycles including pyrazole moieties present a variety of possibilities as chelating agents, since the pyrazole units can behave as monodentate ligands through their sp² nitrogens or as bridged bis(monodentate) η¹:η¹ ligands through deprotonation.²³ Some of us previously showed that transition metals favor the deprotonation of 1*H*-pyrazole rings at the polyamine macrocycle in aqueous solution and at physiological pH, forming Cu(II) or Zn(II) dipyrazolate salts in which the nitrogens acted as exobidentate ligands.^{19,24,25} On the other hand, X-ray diffraction techniques showed that the N-Bn substituted sp² nitrogens of the pyrazole rings in 3 behave as monodentate ligands in the formation of Cu(II) or Zn(II) neutral dinuclear complexes.^{19,25} Other diverse acyclic or cyclic polyamine ligands that are good complexants of transition metals have been used as functional mimics of SOD enzymes,²⁶ and modifying the homeostasis of essential metal ions through the use of metal chelating compounds is a common practice in inorganic medicinal chemistry.²⁷

In this work, we evaluated the effectiveness of compounds 1–4 as selective inhibitors of Fe-SOD in relation to human CuZn-SOD; their in vitro antiparasitic activity and toxicity against Vero cells were tested and compared with values obtained for the reference drug benznidazole (BZN), and on the basis of the results obtained, their in vivo trypanosomicidal activity on female BALB/c mice was measured both in the acute and chronic phase. The effect of compounds 1–4 on the ultrastructure of *T. cruzi* was also studied by transmission electronic microscopy (TEM) experiments in order to confirm the type of damage caused to the parasite cells. A NMR analysis of the nature and percentage of the metabolites excreted was

performed in order to gain some information about the inhibitory effect of our compounds on the glycolytic pathway, since this represents the prime energy source of the parasite. Finally, a histopathological analysis was performed in order to gain better insights into the toxicity levels obtained.

RESULTS AND DISCUSSION

Chemistry. The polyaminic macrocycles 1–4 (Figure 1) were prepared as shown in Scheme 1. Following a procedure previously reported by some of us,¹⁹ the cryptand containing three 1*H*-pyrazole rings (1, mp 244–245 °C from H₂O, 65% yield) was obtained via the condensation of 1*H*-pyrazole-3,5-dicarbaldehyde (5) with tris(2-aminoethyl)amine in methanol and a further in situ reduction of the resulting Schiff base with sodium borohydride. The monocyclic polyamine containing two 1-benzyl-pyrazole units (3) was obtained in two separated steps as also previously reported by us.²¹ In the first step, dipodal [2 + 2] condensation of the previously described 1-benzylpyrazole-3,5-dicarbaldehyde (7)²¹ with 1,5-diamino-3-azapentane in acetonitrile afforded a Schiff base 8 containing two imidazolidine rings located at the pyrazole side close to the benzyl substituents [161–162 °C (EtOH), 55% yield]. After this, the reduction of 8 in the presence of sodium borohydride/ethanol led to the desired polyamine 3 [137–138 °C (toluene), 83% yield]. The related polyamine containing two 3,5-disubstituted 1-methylpyrazole rings (2) had previously been reported as a thick liquid.²⁰ For this work we used an improved method of synthesis and more accurate purification procedures, and were able to isolate compound 2 as a crystalline white solid [mp 133–135 °C (toluene)] in 70% yield. The new method was performed in a unique reaction step via the condensation of 1-methylpyrazole-3,5-dicarbaldehyde with 1,5-diamino-3-azapentane and in situ treatment with sodium borohydride. The polyamine macrocycle *N*-octyl-substituted at the side chains (4) was obtained as previously described²² via the condensation of 1*H*-pyrazole-3,5-dicarbaldehyde with 1,5-diamino-3-octyl-3-azapentane in methanol and in situ treatment with sodium borohydride. After careful chromatographic purification, compound 4 was isolated as a pure syrup with *R*_f 0.54 (TLC, MeOH/30% aqueous NH₄OH, v:v 10:1) with a 53% yield.

Finally, further treatment of compounds 1–4 with HCl in EtOH afforded the corresponding hydrochloride salts 1·8HCl (mp 267–269 °C, 85% yield), 2·6HCl (mp 255–256 °C, 88% yield), 3·6HCl (mp 247–249 °C, 85% yield), and 4·6HCl (mp 230–231 °C, 81% yield) as stable solids. Among them, compounds 2·6HCl and 3·6HCl are described for the first time in this work. Both compounds were unequivocally identified on

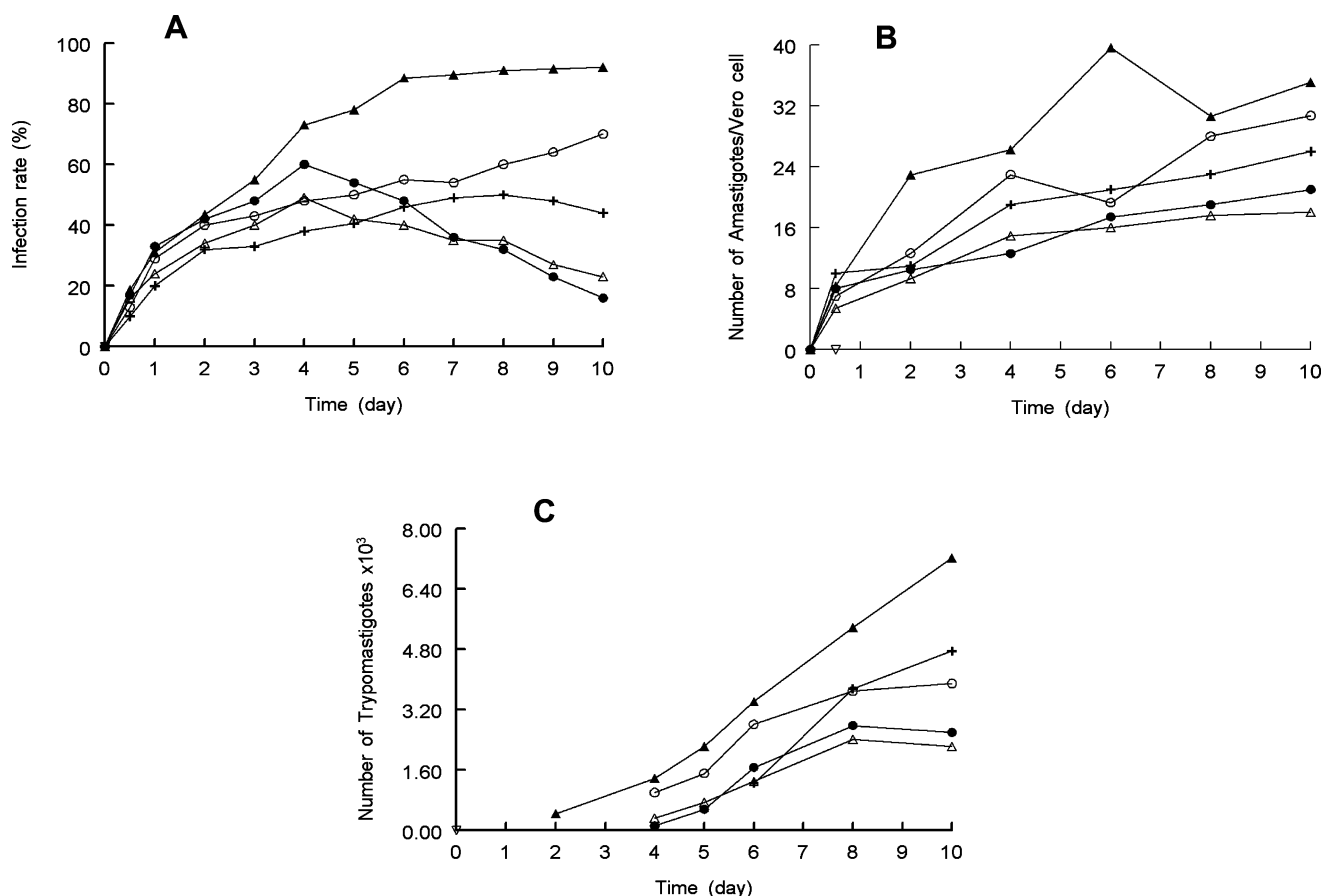


Figure 2. Effect of pyrazole-containing polyamine derivatives 1–3 on the infection rate and growth of *T. cruzi*. (A) Rate of infection, (B) mean number of amastigotes per infected Vero cell, and (C) number of trypomastigotes in the culture medium: (▲) control; (○) BZN; (Δ) compound 1; (●) compound 2; (+) compound 3. Measured at IC_{25} . Values are the means of three separate experiments.

the basis of their analytical data and 1H NMR and ^{13}C NMR spectroscopy. Assignment of the NMR signals was achieved using bidimensional techniques (gHMBC and gHMQC). The ESI mass spectra (positive mode) showed molecular ions corresponding to the proposed structures (m/z 419.4 and 571.5 for 2 and 3, respectively).

In Vitro Anti-*T. cruzi* Evaluation. In the first step, we evaluated the in vitro activity of compounds 1–4 in their hydrochloride forms against *T. cruzi* epimastigotes and amastigotes of an SN3 strain isolated from Colombian *R. prolixus*. Since extracellular epimastigotes are not the developed form of the parasite in vertebrate hosts, assays performed using these are less indicative than assays that use intracellular amastigotes.²⁸ With this in mind, we prepared and tested extracellular epimastigotes and extracellular axenic amastigotes, and in a further step, we infected Vero cells with metacyclic forms of *T. cruzi* that were transformed into amastigotes 1 day after infection. We selected this cell line because it has shown to be a very effective host for *T. cruzi* parasites.

The IC_{50} values obtained for the epimastigotes, axenic amastigotes, and intracellular amastigotes for the test compounds at concentrations of 1–100 μM are shown in the first three columns of Table 1, which also includes the results obtained from the reference drug benznidazole. Toxicity values against mammalian Vero cells after 72 h of culture were also calculated, and the selectivity indexes ($SI = IC_{50}$ Vero cells toxicity/ IC_{50} activity of extracellular or intracellular forms of the parasite) are also shown in the last three columns of Table 1.

We added the number of times that the compound SI exceeded the benznidazole SI, in parentheses, since this value indicates the in vitro potentiality of the test compounds with respect to the reference drug.

If we consider the activity IC_{50} data shown in Table 1, it can be seen that the 1*H*-pyrazole cryptand 1 and the 1-methylpyrazole macrocyclic polyamine 2 were the most active of the four compounds tested in the three assays performed. Furthermore, they were much more active than benznidazole against both the extra- and intracellular forms of the parasite. Next in the activity ranking was the 1-benzylpyrazole derivative 3, whereas the lipophilic polyamine 4, *N*-octyl-substituted in the side chains, was the least active in all cases. Regarding the cytotoxicity evaluation against Vero cells, it was shown that compounds 1–3 were substantially less toxic than the reference drug ($IC_{50} = 149.1, 178.5, \text{ and } 195.4 \mu M$, respectively, against 13.6 μM for benznidazole), and even 4 was slightly less toxic ($IC_{50} = 21.5 \mu M$). Considering now the more illustrative selectivity index values, compounds 1 and 2 were again the most potentially interesting, since their SI values were 143, 30, and 40 times higher than that of benznidazole in the case of 1, and 172, 29, and 46 times higher in the case of 2. Compound 3 was less effective in all cases but, in spite of this, its SI was 15, 28, and 24 times higher than that of BZN, whereas 4 showed SI values very close to those of the reference drug (0.6, 1.4, and 1.8). If we take into account the structural features of the four compounds tested, the bulky and lipophilic macrocycle 4 was clearly the least active of all. When comparing 2 and 3, the *N*-

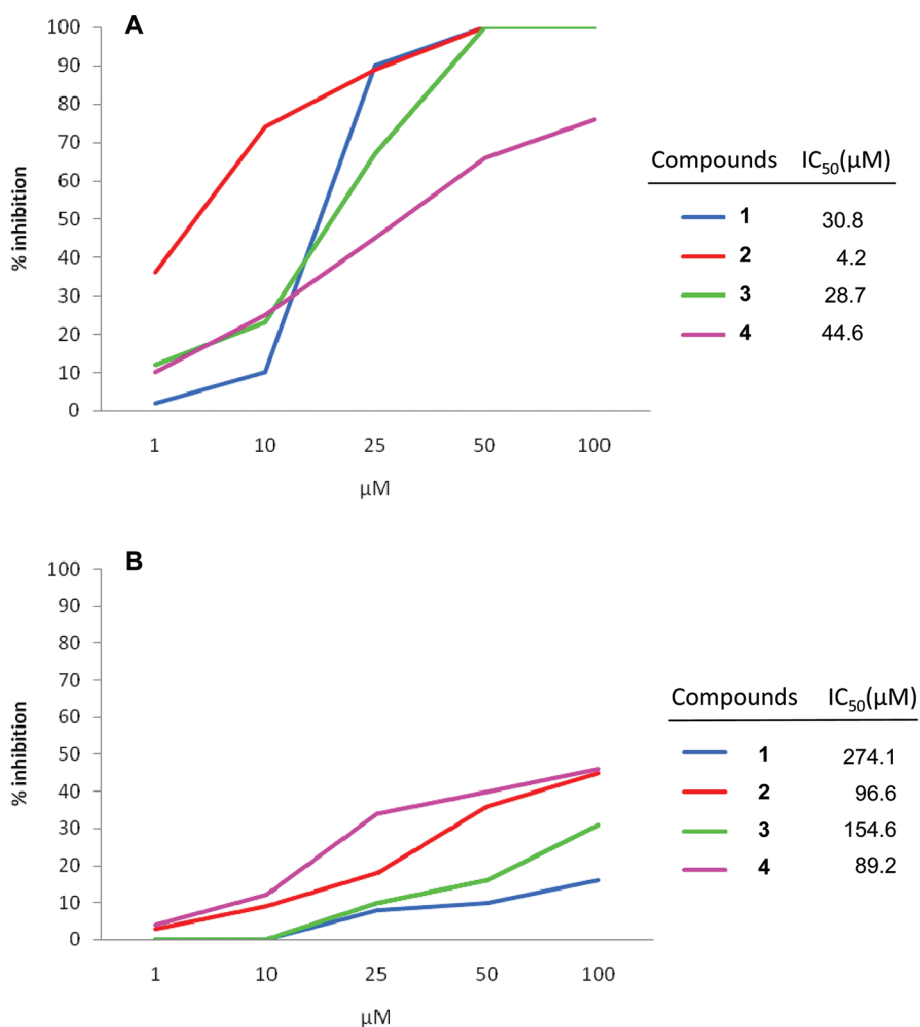


Figure 3. (A) In vitro inhibition (%) of Fe-SOD in *T. cruzi* epimastigotes by compounds 1–4 (activity 20.77 ± 3.18 U/mg). (B) In vitro inhibition of CuZn-SOD in human erythrocytes by compounds 1–4 (activity 23.36 ± 4.21 U/mg). The values are the average of five separate determinations. Differences between the activities of the control homogenate and those incubated with compounds 1–4 were obtained using the Newman–Keuls test. IC₅₀ = the concentration required to give 50% inhibition, which was calculated via linear regression analysis from the K_c values at the concentrations used (1, 10, 25, 50, and 100 μM).

methyl-substituted macrocycle **2**, with the less bulky substituent attached to the pyrazole nitrogen, was clearly more effective than the *N*-benzyl-substituted analog **3**. In summary, the less hindered compounds **1** and **2** appeared to be promising candidates for in vivo assays. After considering the much poorer results obtained from compound **4** and in accordance with the usual protocol, all subsequent assays were exclusively performed with the three compounds that showed the most significant activity in these preliminary tests, with the only exception being those related to the inhibition of parasitic and human SOD enzymes.

In order to achieve more accurate information concerning the in vitro activity of compounds 1–3, the propagation of the parasite in Vero cells was studied by measuring the infection rates and the average number of amastigotes and trypomastigotes present during a 10-day treatment period. Vero cells were incubated for 2 days and then infected with metacyclic forms of *T. cruzi*. The cells were invaded and progressive morphological conversion to the amastigote forms took place. During days 1–10 the rate of host cell infection gradually increased: 92% percent cells were infected on day 10 (Figure 2A). The test was performed again in the presence of each of the three

compounds assayed and also in the presence of the reference drug. It was found that the infection rate decreased in all cases with respect to the control by the end of the test, but not to the same extent. The decrease in the infection rate for compounds 1–3 was always greater than 50%, making them much more effective than benznidazole (23%). Compounds **1** and **2** showed an especially remarkable behavior, with decreases in the infection rate of 74% and 80% respectively, when compared to the control.

The average number of amastigotes increased to a peak on the 6th day of culture and decreased thereafter (Figure 2B); this was because the rupture of Vero cells released amastigotes, which were further transformed into trypomastigotes. The results obtained agreed with those mentioned above for the infection rates. At the end of treatment, the three test compounds had significantly decreased the number of amastigotes present in the cells by 50%, 42%, and 26%, respectively, for **1**, **2**, and **3**, whereas BZN only showed a reduction of 13%. As before, compounds **1** and **2** were clearly more efficient than the bulky *N*-substituted **3**.

Regarding the number of trypomastigotes found in the medium (Figure 2C), a maximum was reached in the control

on day 10 (7.3×10^3), but this value was substantially reduced in the presence of compounds 1 and 2 (70% and 64%, respectively) and was even further reduced in the presence of 3 (34%) and the reference drug (46%). In summary, the Vero cells propagation data showed results that are in accordance with those described for intra- and extracellular forms of *T. cruzi*.

Inhibitory Effect on the *T. cruzi* Fe-SOD Enzyme. Since we had previously found that some benzo[g]phthalazine derivatives are able to complex metal ions and show remarkable inhibitory activity on the antioxidant enzyme Fe-SOD of *T. cruzi*,^{16,17} compounds 1–4 were tested in order to estimate their potential to bind in the active site, thereby inhibiting the enzyme. We used epimastigote forms of *T. cruzi*, which were shown to excrete Fe-SOD when cultured in a medium lacking inactive fetal bovine serum,²⁹ and a range of drug concentrations from 1 to 100 μM was applied in each case. The results obtained are shown in Figure 3A, and the corresponding IC_{50} values were calculated and are included in the same figure. Significant inhibitory values of Fe-SOD activity were found for all compounds tested. Compounds 1–3 showed 98% inhibition at the 50 $\mu\text{g}/\text{mL}$ dose, and even the less active *N*-octyl-substituted polyamine 4 achieved 65% inhibition at the same concentration. Macrocycles 1–3 showed between 70% and 90% inhibition when the 25 $\mu\text{g}/\text{mL}$ dose was used, and the *N*-methyl-substituted macrocycle 2 reached a level of inhibition of 75% at a concentration as low as 10 $\mu\text{g}/\text{mL}$. Figure 3A clearly shows that at lower doses compound 2 was much more effective than 1 and 3, whereas progressively increasing the concentration of the drugs led to a similar effectiveness of 1 and 2 at first and then 1–3, later on. It was also found that the IC_{50} values were more significant in the case of compound 2.

The design of an effective drug able to inhibit the parasite Fe-SOD requires the inhibition of human SOD to occur to a lower extent; therefore, we have also assayed the effect of compounds 1–4 on Cu/Zn-SOD of human erythrocytes (Figure 3B). The results obtained show that the inhibition percentages for human CuZn-SOD were very small for both the higher and lower dosages, with IC_{50} values reaching 274.1, 96.6, 154.6, and 89.2 μM for 1, 2, 3, and 4, respectively, in sharp contrast with the values calculated in part A. All of the compounds tested showed remarkable selectivity in the inhibition of Fe-SOD/CuZn-SOD, but the *N*-methyl-substituted polyamine 2, with an IC_{50} value 23 times higher in the case of Fe-SOD, appeared to be the most effective and most selective compound for Fe-SOD inhibition with respect to human SOD. These results enhance the interest in the potential antiparasitical activity of the macrocyclic polyamines studied in this work and could agree with the hypothesis of some kind of interaction with the iron atom of SOD being one of the feasible mechanisms involved in this activity.

In Vivo Anti-*T. cruzi* Activity. The good results obtained in the *in vitro* tests prompted us to study the *in vivo* activity of compounds 1–3 on female BALB/c mice. Since the effectiveness of drugs currently in use against Chagas disease varies widely from the acute to the chronic phase, we decided to evaluate the impact of our compounds on both phases. For the acute phase experiments, we considered the first 30 days after infection, whereas the effect on the chronic phase was studied between days 40 and 120 after infection. The intraperitoneal doping route was preferred to the intravenous procedure because it is well-known that intraperitoneal treatment substantially reduces animal mortality.³⁰ In fact, no

mouse died in any of our experiments performed either with the control or with compounds 1–3 at the concentrations used (1 mg/kg). However, the survival percentage for the mice treated with BZN was only about 80%. The female mice were inoculated with trypomastigotes using the method described in the Experimental Section, and treatment with the compounds to assay began via the ip route 5 days postinfection and was maintained for 5 days. A group of mice treated in the same manner but only using vehicle (control) was also included. During the study of acute phase activity, the level of parasitemia was determined every 2 days.

Figure 4 shows the number of trypomastigotes against days of treatment until day 30. On the day of the maximum parasitic

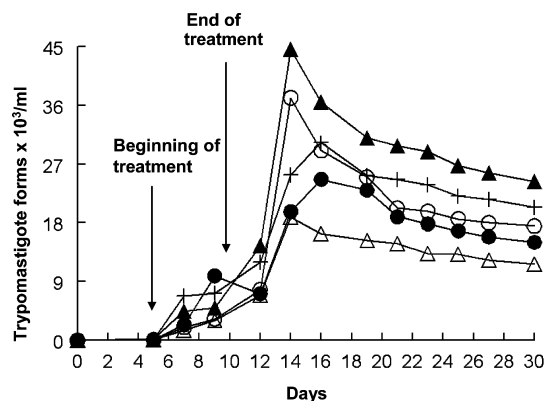


Figure 4. Parasitemia in the murine model of acute Chagas disease: control (▲) mice and mice that received 1 mg/kg doses of BZN (○), compound 1 (Δ), compound 2 (●), and compound 3 (+).

burden (day 14 after infection) all of the test compounds greatly reduced the number of trypomastigotes. Furthermore, it was shown that compounds 1 and 2 reduced the level of parasitemia on day 30 by 53% and 39%, respectively. These values were significantly greater than that found for the reference drug (26%). However, the *N*-benzyl-substituted polyamine 3 was less effective than benznidazole (16%).

Concerning activity in the chronic phase, Table 2 shows the differences found in the level of anti-*T. cruzi* antibodies between

Table 2. Differences in the Level of Anti-*T. cruzi* Antibodies between Days 40 and 120 Postinfection for Compounds 1–3 and BZN, Expressed in Absorbance Units (abs)

compound ^a	ΔA^b
control (untreated)	+0.206
benznidazole	+0.116
1	-0.437
2	-0.291
3	+0.008

^a1 mg/kg/day, intraperitoneal route, administered for 5 days (see Experimental Section). ^b $\Delta A = (\text{absorbance at 490 nm, day 120 postinfection}) - (\text{absorbance at 490 nm, day 40 postinfection})$.

days 40 and 120 postinfection. It was shown that compounds 1 and 2 significantly reduced the levels of antibodies with respect to the control, where the effect of compound 1 was much more consistent. Compound 3 showed a lower performance, but it was still better than that of BZN. The order of *in vivo* activity was as follows: 1 > 2 \gg 3 > BZN. It should be noted that the bicyclic macrocycle 1 was the most effective against both the

acute and chronic phases of Chagas disease. A certain relationship between the structural features of the compounds tested and the trypanosomicidal activity observed can be tentatively proposed if we consider that all of the compounds contain polyaminic moieties that are easy to protonate. We determined the protonation constants of compound **2** at 298.1 K in 0.15 M NaCl and the results obtained were compared to the constants previously calculated for **1** and **3**.^{19,21,31} Plots of the average protonation degree vs pH were calculated from the protonation constants and are collected in the Supporting Information (Table S1 and Figure S1). Figure 5 shows a bar

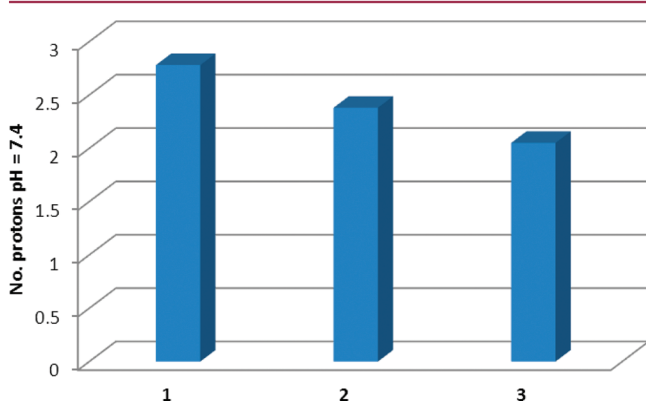


Figure 5. Bar plot of the degree of protonation of compounds **1–3** at pH = 7.4.

plot in which the degree of protonation of the three compounds at physiological pH (7.4) is represented. It is evident from this figure that the order of protonation was $1 > 2 > 3$, so that the protonation ability could, in some way, be conditioning the in vivo activity of these compounds.

Other Studies on the Mechanism of Action. In order to obtain further information about the action mechanisms of compounds **1–3** on the parasite, we performed the following experiments.

Metabolite Excretion Effect. Trypanosomatids depend on the carbon sources present in their hosts for their energy metabolism. Most of them, including *T. cruzi*, mainly use glucose as their energy source, which is abundant in the fluids of vertebrate hosts. At the end of the oxidation process glucose should be totally degraded to CO₂, but the parasite is not able of this under aerobic conditions and excretes a large part of its carbon skeleton into the medium as fermented metabolites at variable grades of oxidation.³² ¹H NMR spectra enable us to determine the fermented metabolites excreted by the trypanosomatid during its in vitro culture, and the use of this technique when a drug has been added to the parasite may provide us with valuable information regarding the metabolic changes induced by the drug. The most significant of the metabolites excreted by *T. cruzi* is succinate, the main role of which could be maintenance of the glycosomal redox balance, since it provides two oxidoreductase enzymes that allow reoxidation of the NADH produced in the glycolytic pathway. The fermentation of succinate is favored because it only requires half the amount of phosphoenolpyruvate (PEP) produced to maintain the NAD⁺/NADH balance. The remaining pyruvate is converted inside the mitochondria³³ mainly in succinate but also into other major catabolites: in *T. cruzi* these metabolites are acetate, L-lactate, L-alanine, and, to a lesser extent, ethanol.

We were interested in evaluating the effect of the macrocyclic polyamines on metabolite excretion; thus, the ¹H NMR spectra obtained from the trypanosomatids treated with compounds **1–4** (Figure 2S in the Supporting Information) were recorded and compared with those obtained from cell-free medium (control) 4 days after inoculation with the *T. cruzi* strain. In the control experiment, the major metabolites excreted by *T. cruzi* were acetate and succinate, with smaller percentages of L-alanine, L-lactate, and ethanol, in agreement with the data in the literature.³⁴ When the trypanosomatids were treated with compounds **1–3**, the excretion of some of these catabolites was neatly altered at the dosage used, whereas the presence of benznidazole did not lead to significant alterations in fuel metabolism. Variation percentages in the height of the signals corresponding to the significant catabolites are shown in Table 3. It can be seen that the excretion of both succinate and acetate

Table 3. Variations in the Percentages of Catabolic End Products Excreted by *T. cruzi* Epimastigotes in the Presence of Compounds **1–3** and Benznidazole Compared to the Control^a

compd	Suc	Ac	Lac	Ala	Et
1	–7	–22	=	=	=
2	–70	–15	–58	=	=
3	–19	–23	=	=	=
BZN	=	+6	=	=	=

^aSuc, succinate; Ac, acetate; Lac, L-lactate; Ala, L-alanine; Et, ethanol; –, peak inhibition; +, peak increasing; =, peak modification undetected.

was inhibited by all three compounds. The excretion of acetate was moderately inhibited from 15% to 23%, which was very similar for all three compounds tested. However, greater variations were found in the inhibition of succinate, the level of which was low for the cryptand **1**, moderate for the *N*-benzyl-substituted polyamine **3**, and surprisingly high (70%) for the *N*-methyl-substituted polyamine **2**, which was also the only compound that inhibited the formation of lactate (58%). Since the less bulky compound **2** showed greater alterations to the level of glucose metabolism of the parasite, and taking into account the relevant role of mitochondria in the formation of the catabolic end products,³⁵ it could be possible that its smaller size allows it to more easily penetrate the cristae (tubular invaginations of the inner mitochondrial membrane)³⁶ leading to subsequent changes in the metabolic pathway. Regarding this point, it should be noted that **2** not only showed greater alterations in glucose catabolism but also that it led to greater levels of Fe-SOD inhibition. Since the Fe-SOD present in mitochondria is an essential part of the whole enzyme excreted by epimastigotes in the inhibition tests,³⁷ this fact would agree with the hypothesis above that this less bulky compound might have a greater ability to pass through the mitochondrial membrane.

Ultrastructural Alterations. The morphological alterations of *T. cruzi* epimastigotes caused by compounds **1–3** were analyzed with transmission electron microscopy (TEM), in order to determine whether or not the post-treatment modifications in the parasite cells could provide more detailed evidence about the way in which the compounds tested affected parasite survival. The most significant variations compared to the control cells are shown in Figure 6. All three compounds caused substantial damage to the parasite cells, and as a rule,

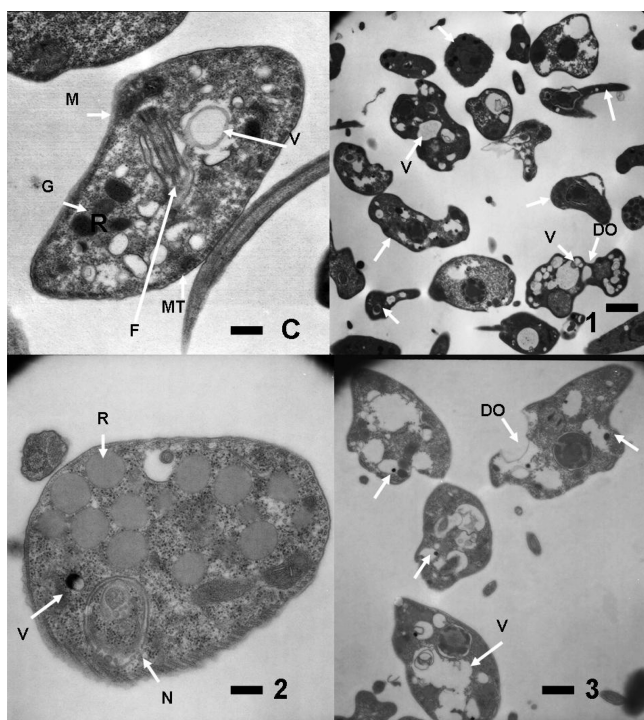


Figure 6. Ultrastructural alterations shown by TEM in epimastigotes of *T. cruzi* treated with compounds 1–3. (Plate C) Control parasite showing organelles with their characteristic features, such as mitochondrion (M), glycosomes (G), microtubules (MT), vacuoles (V), and flagellum (F); bar = 0.583 μm . (Plate 1) Epimastigotes of *T. cruzi* treated with compound 1 with intense vacuolization (V) and very electron dense (arrow) and distorted shapes (DO); bar = 1.590 μm . (Plate 2) Epimastigotes of *T. cruzi* treated with compound 2, with vacuolization (V), cytoplasm full of reservosomes (R), and altered nucleus (N); bar = 0.350 μm . (Plate 3) Epimastigotes of *T. cruzi* treated with compound 3, with vacuolization (V), a distorted shape (DO), and electron-dense sectors (arrow); bar = 1.000 μm .

extensive cytoplasmic vacuolization was observed in all cases. However, cryptand 1 was clearly the most effective (second panel in Figure 6) because it completely altered the morphology of the protozoan cells which, after treatment, showed extremely electron-dense vesicles within both the cytoplasm and the nucleus. The shape of most of the parasites was so distorted that their morphology was completely unrecognizable, and they were also filled with empty vacuoles or membranous structures. Only very few parasites showed a normal appearance, and many were dead. These results were consistent with the predominant *in vivo* activity previously found for 1 compared to the monocyclic polyamines. Although the epimastigotes treated with 2 and 3 clearly showed less damaged, they also presented various morphological alterations that differed depending on the nature of the compound tested. Treatment with the *N*-methyl-substituted polyamine 2 (third panel in Figure 6) resulted in the appearance of reservosomes inside the cytoplasm of the trypanosomatids, and in many cases the nucleus was unrecognizable, presenting a flabby aspect and discontinuous membrane. Many parasites showed extremely electron-dense vesicle-like structures reminiscent of waste products. In turn, the *N*-benzyl-substituted polyamine 3 (fourth panel in Figure 6) induced strong vacuolization of the epimastigotes; furthermore, the vacuoles were occasionally associated, occupying the entire cytoplasm. Sometimes the shape of the parasites was distorted, showing abnormal

indentations and undulations. The presence of electron-dense particles similar to those mentioned in the case of 2 was also observed. Comparing the results obtained for both compounds, the most significant difference found was that modifications in the structure of the membranes were much more substantial for polyamine 2, again in accordance with the lower effectiveness shown by 3 in the *in vivo* activity assays.

In summary, a wide range of ultrastructural alterations to the epimastigote forms of *T. cruzi* treated with compounds 1–3 was found. These alterations, which mainly took place at the mitochondrial and cytoplasmic levels, could be related to the metabolic changes mentioned above concerning the production of succinate and acetate, which might originate from a disturbance in the enzymes involved in pyruvate metabolism inside the cells.

Histopathological Analysis. In order to gain further insights into the level of toxicity induced by our compounds on the liver, a key organ in many vital functions, we performed a histopathological analysis on female BALB/c mice infected with the parasite and treated with compounds 1–3. The results obtained are summarized in Table 4 and shown graphically in

Table 4. Degrees of Histopathological Alteration Found in the Liver of Mice Infected with *T. cruzi*: Untreated and Treated with 5 mg/kg of Benznidazole or Compounds 1–3, after 120 dpi

histopathological alterations	damage level ^a					
	control –	control +	BZN ^b	1	2	3
granulomas with lymphocytic infiltration	+	++++	++	+	+	++
delocalized hepatic destruction	0	++++	++++	+	+	0
blood vessels with thickened walls	+	+++	0	0	++	++
lymphocytic infiltration in the portal tracts	0	++++	0	+	0	++
interstitial hemorrhage	0	++++	++	0	0	++
hepatic destruction in the portal tracts	0	+++	++++	++	+	+
necrotic cells in the portal tracts	0	++++	+++	+	+	0

^aDamage level: + mild; ++ light; +++ moderate; ++++ abundant; +++++ severe. ^bSanchez-Moreno et al.^{17b}

Figure 3S, which can be found in the Supporting Information. We found that mice that were infected but not treated developed severe alterations (control + column) after 120 days compared to uninfected mice (control – column). Those modifications were undoubtedly due to the action of the parasite during the chronic phase. The most remarkable alterations were lymphocytic infiltration with the formation of many microgranulomas (++++), delocalized hepatic destruction (++++), blood vessels with thickened walls (+++), lymphocytic infiltration in the portal tracts (++++), and interstitial hemorrhage (++++). The presence of many necrotic cells in the portal tracts was also detected (++++). In a previous assay^{17b} we found that treatment of parasitized mice with the reference drug (BZN) reduced the formation of granulomas (++), interstitial hemorrhage (++), thickening of blood vessels, and, to a lesser extent, the presence of necrotic cells (+++), due to the lower number of parasites remaining

after drug action. On the contrary, the level of delocalized hepatic destruction was unchanged and very severe hepatic destruction was found in the portal tracts (++++), caused by the BZN toxicity.

After treatment of the infected mice with polyamines 1–3 it was shown that the alterations, as a whole, were not as significant as those mentioned above for BZN, indicating a remarkably lower level of toxicity for the three compounds tested at 120 dpi. Compounds 1 and 2, which were the most active in vivo, generally showed lower levels of damage than compound 3. In both cases all of the aforementioned alterations were nonexistent (0) or mild (+), with the only exceptions being hepatic destruction in the portal tracts (1) and blood vessels thickening (2), which only occurred to a light degree (++) . A strong reduction in the levels of hepatic destruction (both delocalized and in portal tracts) compared to BZN was especially noteworthy for compounds 1 and 2. Even compound 3 showed much better results than BZN regarding the hepatic destruction (mild or none at all).

From the results of this work, we conclude that the macrocyclic polyamines 1 and 2 showed remarkable in vitro and in vivo trypanosomicidal activity, being especially active against both the acute and chronic phases of Chagas disease. These compounds also showed a much lower level of toxicity than benznidazole, as shown by the Vero cell and histopathological studies, and they were almost inactive against human SOD but active against the Fe-SOD of the parasite. On this basis, we believe that both compounds fulfill the requirements needed in order to perform a more detailed study of the nature of the mechanisms involved in their activity patterns, and furthermore, that they are serious candidates for studying parasitological activity at a higher level.

EXPERIMENTAL SECTION

Chemistry. 3,5-Dimethylpyrazole, tris-2-(aminoethyl)amine, and 1,5-diamino-3-azapentane were purchased from commercial sources (Sigma-Aldrich) and used without further purification. 1,5-Diamino-3-octylazapentane is not commercial and was obtained from 1,5-diamino-3-azapentane.²² 1*H*-3,5-pyrazoledicarbaldehyde and 1-benzyl-3,5-dicarbaldehyde were obtained from 3,5-dimethylpyrazole according to a procedure previously described by our research group.²¹ 1-Methyl-3,5-pyrazoledicarbaldehyde was obtained from diethyl 1-methyl-3,5-pyrazoledicarboxylate as described by Kumar et al.²⁰ The solvents were dried using standard techniques.³⁸ All reactions were monitored by thin-layer chromatography (TLC) using DC-Alufolien Silica gel 60PF₂₅₄ (Merck; layer thickness, 0.2 mm). The compounds were detected using UV light (254 nm), iodine, or phosphomolybdic acid. Melting points were determined using a Reichert-Jung hot-stage microscope and are uncorrected. The ¹H and ¹³C NMR spectra were recorded on Varian Inova-300, Varian Inova-400, and Varian Unity-500 spectrometers. The chemical shifts are reported in parts per million (ppm) from tetramethylsilane (TMS), but they were measured against the solvent signals. All assignments were made on the basis of ¹H–¹³C heteronuclear multiple quantum coherence experiments (GHMQC and GHMBC). The electrospray ionization (ESI) mass spectra were registered on a Hewlett-Packard 1100 MSD spectrometer in the electrospray positive mode. The fast atom bombardment (FAB) mass spectra were obtained on a VG AutoSpec spectrometer using a *m*-nitrobenzyl alcohol matrix. Elemental analyses were performed by the Departamento de Análisis, Centro de Química Orgánica “Manuel Lora Tamayo”, CSIC, Madrid, Spain. Elemental analysis was used to ascertain a purity higher than 95% for all of the biologically tested compounds.

Preparation of the Macrocyclic Polyamines 1–4.

1,4,7,8,11,14,17,20,21,24,29,32,33,36-Tetradecaazapentacyclo-[12.12.12]^{6,9,11,19,22,13,31,34}hentetraconta-6,9(41),19(40),21,31,34(39)-

hexaene (1). Pyrazoledicarbaldehyde²¹ (372 mg, 3.0 mmol) was dissolved in warm methanol (180 mL) and added dropwise during 2 h under argon to a stirred solution of tris(2-aminoethyl)amine (292 mg, 2.0 mmol) in methanol (120 mL). After stirring overnight at room temperature, NaBH₄ (340 mg, 9.0 mmol) was added portionwise, and after 2 h the solvent was evaporated to dryness under reduced pressure. The residue was directly recrystallized from water, and the obtained crystals, after drying under vacuum at 80 °C over phosphorus pentoxide, were shown to be the title compound as the monohydrate (381 mg, 65%). Mp: 244–245 °C (lit. mp: 245 °C¹⁹). ¹H NMR (400 MHz, CD₃OD): δ 6.24 (s, 3H, H-4), 3.88 (s, 12H, H-6), 2.90–2.93 (m, 12H, H-7), 2.78–2.81 (m, 12H, H-8) ppm. ¹³C NMR (100 MHz, CD₃OD): δ 147.92 (br s, C-3, C-5), 103.28 (C-4), 54.86 (C-8), 48.54 (C-7), 46.47 (C-6) ppm. MS (FAB) *m/z* (%): 569 (MH⁺, 60). Anal. (C₂₇H₄₈N₁₄·H₂O) C, H, N.

[1]-8*HCl*. A mixture of compound 1 (293.4 mg, 0.5 mmol) and 1 M aqueous hydrochloric acid (4 mL) was stirred for 12 h. After addition of ethanol (50 mL), the crystallized white solid was isolated by filtration and dried over phosphorus pentoxide at 60 °C. Yield: 381 mg (85%). Mp: 267–269 °C (lit. mp: 266–269 °C¹⁹). ¹H NMR (500 MHz, D₂O): δ 6.59 (s, 3H, H-4), 4.27 (s, 12H, H-6), 3.31 (t, 12H, H-7), 2.28 (t, 12H, H-8) ppm. ¹³C NMR (125 MHz, D₂O): δ 140.32 (C-3, C-5), 109.88 (C-4), 51.25 (C-8), 46.24 (C-7), 44.58 (C-6) ppm. Anal. (C₂₇H₄₈N₁₄·8HCl·2H₂O) C, H, N, Cl.

13,26-Dimethyl-3,6,9,12,13,16,19,22,25,26-decaazatricyclo-[22.2.1.1^{11,14}]octacos-1(27),11,14(28),24-tetraene (2).²⁰ A solution of 1-methyl-3,5-pyrazoledicarbaldehyde (6) (276 mg, 2 mmol) in 10 mL of MeCN was added in a dropwise manner, under argon, to a constantly stirred solution of freshly distilled 1,5-diamino-3-azapentane (206 mg, 2 mmol) in 20 mL of the same solvent. After stirring overnight at room temperature, MeOH (40 mL) and sodium borohydride (304 mg, 8 mmol) were added, and after 2 h, the solvent was evaporated to dryness under reduced pressure. Then, 50 mL of CHCl₃ was added, and after stirring for 2 h, the resulting white precipitate (borosodic salts) was filtered and collected. The filtrate was concentrated and the residue was purified by flash column chromatography on silica gel (MeOH/30% aqueous NH₄OH, 49:1 to 46:4). The fractions containing the product of R_f = 0.5 (TLC, MeOH/30% aqueous NH₄OH, 4:1) were combined and evaporated to dryness, and the residue was recrystallized from toluene (8 mL) to give a white solid which was dried over P₂O₅ at 60 °C for 12 h affording 295 mg (70% yield) of 2. Mp: 133–135 °C (lit.: thick oil).²⁰ ¹H NMR (CDCl₃, 400 MHz): δ 6.06 (s, 2H, H-4), 3.75 (s, 6H, N-CH₃), 3.72 (s, 4H, H-6'), 3.71 (s, 4H, H-6), 2.75 (m, 16H, H-7, H-7', H-8, H-8'), 2.19 (br s, 6H, NH) ppm. ¹³C NMR (CDCl₃, 100 MHz): δ 149.86 (C-3), 141.70 (C-5), 104.01 (C-4), 49.16, 49.01, 48.97 (C-7, C-7', C-8, C-8'), 47.18 (C-6), 44.44 (C-6'), 36.06 (N-CH₃) ppm. MS (ESI⁺, MeOH) *m/z* (%): 441.4 (M + Na)⁺, 419.5 (MH)⁺. Anal. (C₂₀H₃₈N₁₀) C, H, N.

[2]-6*HCl*. A mixture of 2 (209 mg, 0.5 mmol) and 1 M aqueous hydrochloric acid (4 mL) was stirred for 12 h. After the addition of ethanol (50 mL), a white solid was formed, filtered off, and dried over phosphorus pentoxide at 60 °C for 48 h. Yield: 296 mg (88%). Mp: 255–256 °C. ¹H NMR (D₂O, 500 MHz): δ 6.68 (s, 2H, H-4), 4.39 (s, 4H, H-6'), 4.21 (s, 4H, H-6), 3.79 (s, 6H, N-CH₃), 3.36 (m, 16H, H-7, H-7', H-8, H-8') ppm. ¹³C NMR (D₂O, 125 MHz): δ 142.27 (C-3), 135.75 (C-5), 111.12 (C-4), 45.24, 45.14 (C-8, C-8'), 45.01 (C-6), 43.56, 43.00 (C-7, C-7'), 42.34 (C-6'), 38.00 (N-CH₃) ppm. MS (ESI⁺, H₂O/HCOOH): *m/z* 419.4 (MH – 6HCl)⁺. Anal. (C₂₀H₃₈N₁₀·6HCl·2H₂O) C, H, N, Cl.

13,26-Dibenzyl-3,6,9,12,13,16,19,22,25,26-decaazapentacyclo-[22.2.1.1^{11,14},0^{2,6},0^{15,19}]octacos-1(27),9,11,14(28),22,24-hexaene (8). A solution of 1-benzyl-3,5-pyrazoledicarbaldehyde (7) (642 mg, 3.0 mmol) in 30 mL of MeCN was added dropwise to a stirring solution of diethylenetriamine (310 mg, 3.0 mmol) in 30 mL of the same solvent. After the mixture was stirred overnight, the Schiff base imidazolidine 8 separated as a thick oil, which solidified after scratching to give a white solid that was crystallized from EtOH (464 mg, 55%). Mp: 161–162 °C (lit. mp: 160–162 °C²¹). ¹H NMR

(CDCl₃, 400 MHz): δ 8.35 (s, 1H, H-6), 8.31 (s, 1H, H-6'), 7.72 (s, 1H, H-4), 7.23 (s, 1H, H-4'), 5.55 (d, 1H, H_A-BnCH₂), 5.54 (d, 1H, H_B-BnCH₂), 5.47 (d, 1H, H_A-Bn'CH₂), 5.40 (d, 1H, H_B-Bn'CH₂), 4.17 (s, 1H, H-9), 4.32 (s, 1H, H-9'), 3.78 (m, 1H, H_A-7), 3.54 (m, 1H, H_B-7), 3.67 (m, 1H, H_A-7'), 3.49 (m, 1H, H_B-7'), 3.05 (m, 1H, H_A-8), 2.51 (m, 1H, H_B-8), 3.01 (m, 1H, H_A-8'), 2.57 (m, 1H, H_B-8'), 3.22 (m, 1H, H_A-10), 3.17 (m, 1H, H_B-10), 3.18 (m, 1H, H_A-10'), 3.12 (m, 1H, H_B-10'), 3.47 (m, 1H, H_A-11), 2.34 (m, 1H, H_B-11), 3.33 (m, 1H, H_A-11'), 2.37 (m, 1H, H_B-11') ppm. ¹³C NMR (CDCl₃, 100 MHz): δ 150.18, 149.99 (C-3, C-3'), 144.70, 145.76 (C-5, C-5'), 105.66, 105.22 (C-4, C-4'), 155.62, 155.37 (C-6, C-6'), 74.78, 74.69 (C-9, C-9'), 59.24, 59.52 (C-7, C-7'), 54.04, 54.34 (C-8, C-8'), 45.18, 45.62 (C-10, C-10'), 52.35, 52.80 (C-11, C-11'), 53.44, 53.42 (C-BnCH₂, C-Bn'CH₂), 137.10, 137.94 (C-Bn *ipso*, C-Bn' *ipso*), 126.73, 126.61 (C-Bn *m*-, C-Bn' *m*-), 128.68, 128.60 (C-Bn *o*-, C-Bn' *o*-), 127.61, 127.49 (C-Bn *p*-, C-Bn' *p*-) ppm. MS (FAB) *m/z* (%): 563 (MH⁺, 54). Anal. (C₃₂H₃₈N₁₀) C, H, N.

13,26-Dibenzyl-3,6,9,12,13,16,19,22,25,26-decaazatricyclo-[22.2.1.1^{11,14}]octacos-1(27),11,14(28),24-tetraene (3). To a stirred suspension of Schiff base **8** (450 mg, 0.8 mmol) in 20 mL of EtOH was added solid NaBH₄ (302 mg, 8.0 mmol) portionwise. The reduction was carried out at room temperature for 2 h. The solvent was then evaporated, and after addition of 20 mL of H₂O, the pH was adjusted to 9 by addition of 5% aqueous HCl. The solution was extracted with CHCl₃, and the organic layer was dried (Na₂SO₄) and evaporated to yield a white solid, which was crystallized from toluene (378 mg, 83%). Mp: 137–138 °C (lit. mp: 136–138 °C²¹). ¹H NMR (D₂O, pH = 12, 400 MHz): δ 7.15 (m, 6H, H-Bn *m*-, *p*-), 6.97 (m, 4H, H-Bn *o*-), 6.17 (s, 2H, H₄), 5.17 (s, 4H, H-BnCH₂), 3.57 (s, 8H, H-6, H-6'), 2.41 (s, 8H, H-7, H-7'), 2.32 (t, 4H, H-8), 2.23 (t, 4H, H-8') ppm. ¹³C NMR (D₂O, pH 12, 75 MHz): δ 150.75 (C-3), 143.70 (C-5), 138.03 (C-Bn *ipso*), 130.02 (C-Bn *o*-), 127.64 (C-Bn *m*-), 129.05 (C-Bn *p*-), 106.34 (C-4), 53.20 (C-BnCH₂), 47.14 (C-7, C-7'), 48.15 (C-8), 46.73 (C-8'), 45.90 (C-6), 43.42 (C-6') ppm. MS (FAB) *m/z* (%): 571 (MH⁺, 69). Anal. (C₃₂H₄₆N₁₀) C, H, N.

[3]-6HCl. A mixture of **3** (285 mg, 0.5 mmol) and 1 M aqueous hydrochloric acid (4 mL) was stirred for 12 h. After the addition of ethanol (50 mL), a white solid was formed, filtered off, and dried over phosphorus pentoxide at 60 °C for 48 h. Yield: 350 mg (85%). Mp: 247–249 °C. ¹H NMR (D₂O, 400 MHz): δ 7.28 (m, 6H, H-Bn *m*-, H-Bn *p*-), 7.01 (m, 4H, H-Bn *o*-), 6.78 (s, 2H, H-4), 5.40 (s, 4H, H-BnCH₂), 4.35 (s, 4H, H-6'), 4.26 (s, 4H, H-6), 3.35–3.40 (m, 8H, H-7', H-8') 3.30–3.35 (m, 8H, H-7, H-8) ppm. ¹³C NMR (CDCl₃, 75 MHz): δ 143.22 (C-3), 136.21, 136.82 (C-5, C-Bn *ipso*: interchangeable signals), 130.44 (C-Bn *m*-), 129.70 (C-Bn *p*-), 128.10 (C-Bn *o*-), 111.23 (C-4), 54.58 (C-BnCH₂), 45.30 (C-6), 45.20 (C-8'), 45.14 (C-7') 43.75, 43.19 (C-7, C-8: interchangeable signals), 42.56 (C-6') ppm. MS (ESI⁺, H₂O/HCOOH) *m/z* positive mode (%): 571.5 (MH – 6HCl)⁺. Anal. (C₃₂H₄₆N₁₀·6HCl·2H₂O) C, H, N, Cl.

6,19-Dioctyl-3,6,9,12,13,16,19,22,25,26-decaazatricyclo-[22.2.1.1^{11,14}]octacos-1(27),11,14(28),24-tetraene (4). 3,5-Pyrazole-dicarbaldehyde (372 mg, 3 mmol) was dissolved in hot methanol (180 mL). This solution was then cooled to room temperature and added dropwise under argon to a stirred solution of 1,5-diamine-3-octyl-3-azapentane²² (646 mg, 3 mmol) in methanol (300 mL). The reaction was monitored by TLC (Cl₃CH/MeOH 10:1), and when it was complete (ca. 12 h), NaBH₄ (681 mg, 18 mmol) was added portionwise. After 2 h of reaction, the solvent was evaporated to dryness under reduced pressure. The residual syrup was purified by flash column chromatography on silica gel (MeOH/30% aqueous NH₃, 48:2). The free macrocycle was obtained as a colorless syrup. TLC: *R_f* = 0.54, MeOH/30% aqueous NH₄OH 10:1. Yield: 517 mg (53%). ¹H NMR (CDCl₃, 400 MHz): δ 6.11 (s, 2H, H-4), 3.81 (s, 8H, H-6), 2.84 (m, 8H, H-7), 2.65 (m, 8H, H-8), 2.48 (m, 4H, H-1 octyl), 1.41 (m, 4H, H-2 octyl), 1.21 (m, 20H, H-3 octyl, H-4 octyl, H-5 octyl, H-6 octyl, H-7 octyl), 0.83 (t, 6H, H-8 octyl) ppm. ¹³C NMR (CDCl₃, 100 MHz): δ 145.67 (C-3, C-5), 102.47 (C-4), 54.18 (C-1 octyl), 51.29 (C-8), 46.98 (C-7), 45.30 (C-6), 31.79 (C-6 octyl), 29.49, 29.25, 27.51, 25.88 (C-2 octyl, C-3 octyl, C-4 octyl, C-5 octyl), 22.6 (C-7

octyl), 14.1 (C-8 octyl) ppm. MS (ESI⁺, MeOH) *m/z* (%): 616 (MH⁺). Anal. (C₃₄H₆₆N₁₀·2H₂O) C, H, N.

[4]-6HCl. A mixture of compound **4** (326 mg, 0.5 mmol) and 1 M aqueous HCl (3 mL) was stirred for 12 h. After addition of EtOH (50 mL), the solvent was evaporated to dryness. Next, 30 mL of EtOH was added, and the resulting solution was stirred for 1 h. A white solid was formed, filtered off, and dried over phosphorus pentoxide at 60 °C for 48 h. Yield: 337 mg (81%). Mp: 230–231 °C (lit. mp:²² 228–231 °C). ¹H NMR (D₂O, 400 MHz): δ 6.57 (s, 2H, H-4), 4.22 (s, 8H, H-6), 3.36 (m, 8H, H-8), 3.30 (m, 8H, H-7), 3.04 (t, 4H, H-1 octyl), 3.22 (m, 4H, H-2 octyl), 1.06 (m, 10H, H-3 octyl, H-4 octyl, H-5 octyl, H-6 octyl, H-7 octyl), 0.61 (t, 6H, H-8 octyl) ppm. ¹³C NMR (D₂O, 100 MHz): δ 139.68 (C-3, C-5), 110.18 (C-4), 55.52 (C-1 octyl), 49.87 (C-8), 43.89 (C-6), 41.81 (C-7), 32.11 (C-6 octyl), 29.33 (C-4 octyl, C-5 octyl), 26.73 (C-3 octyl), 23.97 (C-2 octyl), 23.13 (C-7 octyl), 14.55 (C-8 octyl) ppm. MS (ESI⁺, H₂O): *m/z* 616 ([MH – 6HCl]⁺). Anal. (C₃₄H₆₆N₁₀·6HCl) C, H, N.

Parasite Strain, Culture. *T. cruzi* SN3 strain of IRHOD/CO/2008/SH3 was isolated from domestic *R. prolixus*, the biological origin of which is Guajira, Colombia.³⁹ Epimastigote forms were grown in axenic Grace's insect medium (Gibco) supplemented with 10% inactivated fetal bovine serum (FBS) at 28 °C in tissue-culture flasks. In order to obtain the parasite suspension for the trypanocidal assay, the epimastigote culture (in the exponential growth phase) was concentrated by centrifugation at 400g for 10 min and the number of flagellates was counted in a hemocytometric chamber.

Transformation of Epimastigotes to the Metacyclic Form. Metacyclogenesis was induced by culturing the parasites at 28 °C in modified Grace's medium (Gibco) for 12 days, as described previously.⁴⁰ Twelve days after cultivation at 28 °C, metacyclic forms were counted in a Neubauer hemocytometric chamber. The proportion of metacyclic forms was around 40% at this stage.

Cell Culture and Cytotoxicity Tests. Vero cells (Flow) were grown in RPMI (Gibco), supplemented with 10% inactivated fetal bovine serum, in a humidified 95% air, 5% CO₂ atmosphere at 37 °C for 2 days. For the cytotoxicity testing, cells were placed in 25 mL Colie-based bottles (Sterling) and centrifuged at 100g for 5 min. The culture medium was removed, and fresh medium was added to a final concentration of 1 × 10⁵ cells/mL. This cell suspension was distributed in a culture tray (with 24 wells) at a rate of 100 μL/well and incubated for 2 days at 37 °C in a humidified atmosphere enriched with 5% CO₂. The medium was removed, and fresh medium was added together with each test compound (at concentrations of 100, 50, 25, 10, and 1 μM). After 72 h of treatment, cell viability was determined by flow cytometry according to a methodology described by us.⁴¹

In Vitro Activity Assays: Extracellular Forms. *Epimastigote Assay.* Epimastigotes were collected in the exponential growth phase and distributed in culture trays (with 24 wells) at a final concentration of 5 × 10⁴ parasites/well. The compounds to be tested and benznidazole were dissolved in medium trypanosomes liquid (MTL) and were tested at 100, 50, 25, 10, and 1 μM. The effects of the different concentrations of each compound against the epimastigotes were tested for 72 h using a Neubauer hemocytometric chamber. The trypanocidal effect is expressed as IC₅₀ values, i.e., the concentration required to result in 50% inhibition, as calculated by linear-regression analysis from the K_c values of the concentrations used.

In Vitro Activity Assays: Intracellular Forms. *Axenic Amastigotes Assay.* Axenic amastigotes of *T. cruzi*, were cultured following the methodology described previously by Moreno et al.⁴² Thus, the epimastigote transformation to amastigotes was achieved after 3 days of culture in M199 medium (Invitrogen, Leiden, The Netherlands) supplemented with 10% heat-inactivated FCS, 1 g/L β-alanine, 100 mg/L L-asparagine, 200 mg/L saccharose, 50 mg/L sodium pyruvate, 320 mg/L malic acid, 40 mg/L fumaric acid, 70 mg/L succinic acid, 200 mg/L α-ketoglutaric acid, 300 mg/L citric acid, 1.1 g/L sodium bicarbonate, 5 g/L MES, 0.4 mg/L hemin, and 10 mg/L gentamicine, pH 5.4 at 37 °C. The effect of each compound

against the axenic amastigotes was tested for 48 h using a Neubauer hemocytometric chamber. The trypanocidal effect is expressed as IC_{50} values, i.e., the concentration required to result in 50% inhibition, as calculated by linear-regression analysis from the K_c values of the concentrations used.

Amastigotes Assay. Vero cells were cultured in RPMI medium in a humidified 95% air and 5% CO_2 atmosphere at 37 °C. The cells were seeded at a density of 1×10^4 cells/well in 24-well microplates (Nunc) with rounded coverslips on the bottom and then cultivated for 2 days. Afterward, adhered Vero cells were infected in vitro with metacyclic forms of *T. cruzi*, at a ratio of 10:1 and maintained for 24 h at 37 °C in 5% CO_2 in air. The extracellular parasites were removed by washing, and the infected cultures were incubated with the compounds (1, 10, 25, 50, and 100 μM concentrations) and cultured for 72 h in RPMI and 10% inactivated fetal bovine serum. The activity of the compounds was determined from the percentage reduction in the number of amastigotes in the treated and untreated cultures in methanol-fixed and Giemsa-stained preparations. The values are the means of four separate determinations.⁴³ The trypanocidal effect was expressed as IC_{50} values.

Infectivity Assay. The Vero cells were cultured in RPMI medium as described above. Afterward, the cells were infected in vitro with metacyclic forms of *T. cruzi* at a ratio of 10:1. The test compounds (IC_{25} concentrations) were added immediately after infection and incubated for 12 h at 37 °C in a 5% CO_2 atmosphere. The extracellular parasites and the test compounds were removed by washing and the infected cultures were grown for 10 days in fresh medium. Fresh culture medium was added every 48 h. The activity of each compound tested was determined from the percentage of infected cells and the number of amastigotes per infected cell in treated and untreated cultures in the methanol-fixed and Giemsa-stained preparations. The percentage of infected cells and the mean number of amastigotes per infected cell were determined by analyzing more than 100 host cells distributed throughout randomly chosen microscopic fields. The values are the means of four separate determinations. The number of trypanomastigotes in the medium was determined as previously described.⁴⁰

SOD Enzymatic Inhibition. The parasites cultured as described above were centrifuged. The pellet was suspended in 3 mL of STE buffer (0.25 M sucrose, 25 mM Tris-HCl, 1 M EDTA, pH 7.8) and disrupted by three cycles of sonic disintegration, 30 s each at 60 V. The sonicated homogenate was centrifuged at 1500g for 5 min at 4 °C, and the pellet was washed three times in ice-cold STE buffer. This fraction was centrifuged (2500g for 10 min at 4 °C) and the supernatant was collected. The protein concentrations were determined using the Bradford method.⁴⁴ Iron and copper-zinc superoxide dismutases (Fe-SOD and CuZn-SOD) activities were determined using the method described by Beyer and Fridovich,⁴⁵ which measures the reduction in nitroblue tetrazolium (NBT) by superoxide ions. Into each bucket was added 845 μL of stock solution [3 mL of L-methionine (300 mg, 10 mL⁻¹), 2 mL of NBT (1.41 mg, 10 mL⁻¹) and 1.5 mL of Triton X-100 1% (v/v)], along with 30 μL of the parasite homogenate fraction, 10 μL of riboflavine (0.44 mg, 10 mL⁻¹), and an equivalent volume of the different concentrations of the compounds tested. Five different concentrations were used for each product: 1, 2.5, 5, 12.5, and 25 μM (equivalent to 5, 12.5, 25, 62, and 125 μL , respectively, of the stock solution). In the control experiment the volume was made up to 1000 μL with 50 mM potassium phosphate buffer (pH 7.8, 3 mL), whereas 30 μL of the parasite homogenate fraction was added to the mixtures containing the compounds. Then, the absorbance (A_0) was measured at 560 nm in a spectrophotometer. Following this, each bucket was illuminated with UV light for 10 min under constant stirring and the absorbance (A_1) was measured. The human CuZn-SOD, coenzymes and substrates used in these assays were obtained from Sigma Chemical Co. The data obtained were analyzed using the Newman-Keuls test.

In Vivo Trypanosomicidal Activity Assay. Groups of three BALB/c female mice (6–8 weeks old; 20–25 g), maintained under standard conditions, were infected (bloodstream) with 1×10^5 metacyclic forms of *T. cruzi* via the intraperitoneal route. The animals

were divided into the following groups: (1) uninfected (not infected and not treated), (2) untreated (infected with *T. cruzi* but not treated), (3) uninfected [not infected but treated with 1 mg/kg body weight/day, for 5 consecutive days (5–10 days postinfection) via the intraperitoneal route],⁴⁶ and (4) treated [infected and treated for 5 consecutive days (5–10 days postinfection) with the test compounds and benznidazole]. This animal experiment was performed with the approval of an ethical committee of the University of Granada. Treatments were started 5 days after the animals were infected. The compounds were administered in a similar way as explained above and at the same concentrations. A blood sample (5 μL) drawn from the mandibular vein of each treated mouse was taken and diluted at a ratio of 1:15 with 50 μL of 0.1 M citrate buffer: citric acid, 0.1 M sodium citrate, and 20 μL of lysis buffer at pH 7.2. The parasites were counted using an immersion objective. The number of metacyclic forms of *T. cruzi* in the bloodstream was recorded every 2 days from 5 to 30 days postinfection. The number of metacyclic forms was expressed as parasites/mL. Circulating anti-*T. cruzi* antibodies on days 40 and 120 postinfection were quantitatively evaluated using an enzyme-linked immunoassay. The blood, diluted to 1:50 in PBS, was reacted with an antigen composed of an excreted Fe-SOD of *T. cruzi* epimastigotes. The results were expressed as the ratio of the absorbance of each sample at 490 nm to the cutoff value. The cutoff point for each reaction was the mean of the values determined for the negative controls plus 3 times the standard deviation.⁴⁷

Metabolite Excretion. Cultures of *T. cruzi* epimastigotes (initial concentration 5×10^5 cells/mL) received IC_{25} of the compounds (except for the control cultures). After incubation for 96 h at 28 °C, the cells were centrifuged at 400g for 10 min. The supernatants were collected in order to determine the excreted metabolites through ¹H NMR, and the chemical shifts were expressed in parts per million (ppm), using sodium 2,2-dimethyl-2-silapentane-5-sulfonate as the reference signal. The chemical displacements used to identify the respective metabolites were consistent with those described by us.⁴⁸

Ultrastructural Alterations. The parasites were cultured at a density of 5×10^5 cells/mL in each corresponding medium containing the compounds tested at the concentration of IC_{25} . After 96 h, these cultures were centrifuged at 400g for 10 min, and the pellets produced were washed in PBS and then mixed with 2% (v/v) *p*-formaldehyde/glutaraldehyde in 0.05 M cacodylate buffer (pH 7.4) for 4 h at 4 °C. Following this, the pellets were prepared for transmission electron microscopy study using a technique described by us.⁴³

Histopathological Analysis. The liver was extracted from each mouse 120 days postinfection, cut longitudinally, rinsed in ice-cold PBS, and fixed in 10% buffered formalin. The tissues were dehydrated and embedded in paraffin. Sections were cut at a thickness of 4–5 μm and stained with hematoxylin–eosin (H&E) and Masson's trichrome-staining protocol (Trichrome). The slides were coded for a blinded analysis. Histological examinations were performed using a conventional light microscope; each slide was visualized in at least 30 fields (total magnifications: $\times 40$, $\times 100$, $\times 200$, and $\times 400$). The histological alterations were given a score of 0 (–) to 5 (++++), with 0 representing a complete absence of alterations and 5 representing the most severe alterations.

■ ASSOCIATED CONTENT

📄 Supporting Information

Details on the combustion analysis, the protonation constants and the degrees of protonation at pH 2–12, the NMR spectra obtained from the metabolite excretion studies, and details of the histopathological analysis. This material is available free of charge via the Internet at <http://pubs.acs.org>.

■ AUTHOR INFORMATION

Corresponding Author

*M.S.-M.: phone, +34-958-242-369; fax: +34-958-243-862; e-mail: msanchem@ugr.es. P.N.: phone: +34-91-258-7572; fax: +34-91-564-4853; e-mail: iqmnt38@iqm.csic.es. E.G.-E.:

phone: +34-963-544879; fax: +34-96-354-3274; e-mail: Enrique.Garcia-Es@uv.es.

Notes

The authors declare no competing financial interest.

ACKNOWLEDGMENTS

The authors thank the MCINN Projects: Consolider Ingenio CSD2010-00065 and CTQ2009-14288-C04-01, the FEDER funds and Generalitat Valenciana PROMETEO 2011/008, the Santander-Universidad Complutense Research Program GR58/08-921371-891, and the Spanish MEC Project CGL2008-03687-E/BOS for financial support. J.P. thanks MCINN for a predoctoral fellowship. We are also grateful to the NMR and Elemental Analysis Services of the Centro Nacional de Química Orgánica Manuel Lora-Tamayo (C.S.I.C) and also to the Transmission-Electron Microscopy and Nuclear Magnetic Resonance Spectroscopy Services of the CIC-University of Granada.

ABBREVIATIONS USED

SOD, superoxide dismutase; WHO, World Health Organization; BZN, benzimidazole; TEM, transmission electron microscopy; HMQC, heteronuclear single quantum coherence experiment; HMBC, heteronuclear multiple bond coherence experiment; ESI, electrospray ionization; SI, selectivity index; dpi, days postinfection; TLC, thin-layer chromatography; TMS, tetramethylsilane; MEM, minimal essential medium; NAD(P)-H, nicotinamide adenine dinucleotide phosphate; PEP, phosphoenolpyruvate; FAB, fast atom bombardment; FBS, fetal bovine serum; MTL, medium trypanosomes liquid; EDTA, ethylenediaminetetraacetic acid; MES, 4-morpholinethanesulfonic acid; NBT, nitroblue tetrazolium; PBS, phosphate-buffered saline solution

REFERENCES

- (1) Hotez, P. J.; Molyneux, D. H.; Fenwick, A.; Kumaresan, J.; Ehrlich-Sachs, S.; Sachs, J. D.; Savioli, L. Control of neglected tropical diseases. *N. Engl. J. Med.* **2007**, *357*, 1018–1027.
- (2) Zeledon, R.; Rabinovich, J. E. Chagas disease: An ecological appraisal with special emphasis on its insect vectors. *Annu. Rev. Entomol.* **1981**, *26*, 101–133.
- (3) Schmunis, G. A. Prevention of transfusional *Trypanosoma cruzi* infection in Latin America. *Mem. Inst. Oswaldo Cruz* **1999**, *94*, 93–101.
- (4) Torrico, F.; Alonso-Vega, C.; Suarez, E.; Rodriguez, P.; Torrico, M. C.; Dramaix, M.; Truyens, C.; Carlier, Y. Maternal *Trypanosoma cruzi* infection, pregnancy outcome, morbidity, and mortality of congenitally infected and non-infected new borns in Bolivia. *Am. J. Trop. Med. Hyg.* **2004**, *70*, 201–209.
- (5) Pereira, K. S.; Schmidt, F. L.; Guaraldo, A. M.; Franco, R. M.; Dias, V. L.; Passos, L. A. Chagas disease as a foodborne illness. *J. Food Prot.* **2009**, *72*, 441–446.
- (6) Strosberg, A. M.; Barrio, K.; Stinger, V. H.; Tashker, J.; Wilbur, J. C.; Wilson, L.; Woo, K. Chagas disease: A Latin American nemesis. *Institute for One World Health (IOWH), Technical Report* **2007**, 1–110.
- (7) Gascon, J.; Bern, C.; Pinazo, M. J. Chagas disease in Spain, the United States, and other non-endemic countries. *Acta Trop.* **2010**, *115*, 22–27.
- (8) Rassi, A., jr.; Rassi, A.; Marin-Neto, J. A. Chagas disease. *Lancet* **2010**, *375*, 1388–1402.
- (9) (a) Rodrigues-Coura, J.; de Castro, S. L. A critical review on Chagas disease chemotherapy. *Mem. Inst. Oswaldo Cruz, Part A* **2002**, *97* (1), 3–24. (b) Dias, J. C. P. Natural history of Chagas disease. *Arq. Bras. Cardiol.* **1995**, *65*, 359–366.
- (10) Urbina, J. A. Chemotherapy of Chagas disease. *Curr. Pharm. Des.* **2002**, *8* (4), 287–295.

- (11) Viotti, R.; Vigliano, C.; Lococo, B.; Alvarez, M. G.; Petti, M.; Bertocchi, G.; Armenti, A. Side effects of benzimidazole as treatment in chronic Chagas disease: Fears and realities. *Expert Rev. Anti. Infect. Ther.* **2009**, *7*, 157–163.

- (12) Schofield, C. J.; Jannin, J.; Salvatella, R. The future of Chagas disease control. *Trends Parasitol.* **2006**, *22* (12), 583–588.

- (13) (a) Maya, J. D.; Cassels, D. K.; Iturriaga-Vasquez, P.; Ferreira, J.; Faúndez, M.; Galanti, N.; Ferreira, A.; Morello, A. Mode of action of natural and synthetic drugs against *Trypanosoma cruzi* and their interaction with the mammalian host. *Comp. Biochem. Physiol. A Mol. Integr. Physiol.* **2007**, *146* (4), 601–620. (b) Wilkinson, S. R.; Bot, C.; Kelly, J. M.; Hall, B. S. Trypanocidal activity of nitroaromatic prodrugs: Current treatments and future perspectives. *Curr. Top. Med. Chem.* **2011**, *11* (16), 2072–2084.

- (14) (a) Mehlotra, R. K. Antioxidant defense mechanisms in parasitic protozoa. *Crit. Rev. Microbiol.* **1996**, *22* (4), 295–314. (b) Atwood, J. A.; Weatherly, D. B., 3rd; Minning, T. A.; Bundy, B.; Cavola, C.; Oppendoes, F. R.; Orlando, R.; Tarleton, R. L. The *Trypanosoma cruzi* proteome. *Science* **2005**, *309*, 473–476.

- (15) Ghosh, S.; Goswami, S.; Adhya, S. Role of superoxide dismutase in survival of *Leishmania* within the macrophage. *Biochem. J.* **2003**, *369*, 447–452.

- (16) Rodriguez-Ciria, M.; Sanz, A. M.; Yunta, M. J. R.; Gomez-Conteras, F.; Navarro, P.; Sanchez-Moreno, M.; Boutaleb-Charki, S.; Osuna, A.; Castiñeiras, A.; Pardo, M.; Cano, C.; Campayo, L. 1,4-Bis(alkylamino)benzo[g]phthalazines able to form complexes of Cu(II) which as free ligands behave as SOD inhibitors and show efficient in vitro activity against *Trypanosoma cruzi*. *Bioorg. Med. Chem.* **2007**, *15*, 2081–2091.

- (17) (a) Sanz, A. M.; Gomez-Conteras, F.; Navarro, P.; Sánchez-Moreno, M.; Boutaleb-Charki, S.; Campuzano, J.; Pardo, M.; Osuna, A.; Cano, C.; Yunta, M. J. R.; Campayo, L. Efficient inhibition of Fe-SOD and of *Trypanosoma cruzi* growth by benzo[g]phthalazine derivatives functionalized with one or two imidazole rings. *J. Med. Chem.* **2008**, *51* (6), 1962–1966. (b) Sánchez-Moreno, M.; Sanz, A. M.; Gomez-Conteras, F.; Navarro, P.; Marín, C.; Ramírez-Macías, I.; Rosales, M. J.; Olmo, F.; García-Aranda, I.; Campayo, L.; Cano, C.; Arrebola, F.; Yunta, M. J. R. In vivo trypanosomicidal activity of imidazole- or pyrazole-based benzo[g]phthalazine derivatives against acute and chronic phases of Chagas disease. *J. Med. Chem.* **2011**, *54*, 970–979.

- (18) Kumar, M.; Arán, V. J.; Navarro, P. New proton ionizable 3,5-disubstituted pyrazole cryptands able to form tripyrazolate-derived di- and tetra-nuclear complexes of Cu²⁺ and Zn²⁺. *Tetrahedron Lett.* **1995**, *36*, 2161–2164.

- (19) Lamarque, L.; Navarro, P.; Miranda, C.; Arán, J. V.; Ochoa, C.; Escartí, F.; García-España, E.; Latorre, J.; Luis, S. V.; Miravet, J. F. Dopamine interaction in the absence and in the presence of Cu²⁺ ions with macrocyclic and macrobicyclic polyamines containing pyrazole units. Crystal structure of [Cu₂(L₁)(H₂O)₂](ClO₄)₄ and [Cu₂(H₋₁L₃)](ClO₄)₃·2H₂O. *J. Am. Chem. Soc.* **2001**, *123*, 10560–10570.

- (20) Kumar, M.; Bhalla, V. S. N.; Kumar, V.; Singh, M.; Singh, G. J. *Incl. Phenom. Macrocycl. Chem.* **2001**, *39*, 241–245.

- (21) Arán, V. J.; Kumar, M.; Molina, J.; Lamarque, L.; Navarro, P.; García-España, E.; Ramirez, J. A.; Luis, S. V.; Escuder, B. Synthesis and protonation behavior of 26-membered oxaza- and polyaza- macrocycles containing two heteroaromatic units of 3,5-disubstituted pyrazole or 1-benzylpyrazole: A potentiometric and ¹H and ¹³C NMR study. *J. Org. Chem.* **1999**, *64* (17), 6135–6146.

- (22) Miranda, C.; Escartí, F.; Lamarque, L.; Yunta, M. J. R.; Navarro, P.; García-España, E.; Jimeno, M. L. New 1H-pyrazole-containing polyamine receptors able to complex L-glutamate in water at physiological pH values. *J. Am. Chem. Soc.* **2004**, *126*, 823–833.

- (23) Klingele, J.; Dechert, S.; Meyer, F. Polynuclear transition metal complexes of metal-metal-bridging compartmental pyrazolate ligands. *Coord. Chem. Rev.* **2009**, *253*, 2698–2741.

- (24) Lamarque, L.; Miranda, C.; Navarro, P.; Escartí, F.; García-España, E.; Latorre, J.; Ramirez, J. A. Dopamine interaction with a

polyamine cryptand of 1*H*-pyrazole in the absence and in the presence of Cu(II) Ions. Crystal structure of [Cu₂(H₋₁L)](ClO₄)₃·2H₂O. *Chem. Commun.* **2000**, 1337–1338.

(25) Miranda, C.; Escartí, F.; Lamarque, L.; García-España, E.; Navarro, P.; Latorre, J.; Lloret, F.; Jiménez, H. R.; Yunta, M. J. R. Cu^{II} and Zn^{II} coordination of pyrazole-containing polyamine receptors: Influence of the hydrocarbon side chain length on the metal coordination. *Eur. J. Inorg. Chem.* **2005**, 189–208.

(26) Riley, D. P. Functional mimics of superoxide dismutase enzymes as therapeutic agents. *Chem. Rev.* **1999**, 99, 2573–2587.

(27) Orvig, C.; Abrams, M. J. Medicinal inorganic chemistry: Introduction. *Chem. Rev.* **1999**, 99, 2201–2203.

(28) González, P.; Marín, C.; Rodríguez-González, I.; Hitos, A. B.; Rosales, M. J.; Reina, M.; Díaz, J. G.; González-Coloma, A.; Sánchez-Moreno, M. In vitro activity of C₂₀-diterpenoid alkaloid derivatives in promastigotes and intracellular amastigotes of *Leishmania infantum*. *Int. J. Antimicrob. Agents* **2005**, 25, 136–141.

(29) Villagran, M. E.; Marín, C.; Rodríguez-González, I.; de Diego, J. A.; Sanchez-Moreno, M. Use of an iron superoxide dismutase excreted by *Trypanosoma cruzi* in the diagnosis of Chagas disease: Seroprevalence in rural zones of the state of Queretato, Mexico. *Am. J. Trop. Med. Hyg.* **2005**, 73, 510–516.

(30) Da Silva, C. F.; Batista, M. M.; Batista, D. G. J.; de Souza, E. M.; da Silva, P. B.; de Oliveira, G. M.; Meuser, A. S.; Shareef, A. R.; Boykin, D. W.; Soeiro, M. N. C. In vitro and in vivo studies of the trypanocidal activity of a diarylthiophene diamidine against *Trypanosoma cruzi*. *Antimicrob. Agents Chemother.* **2008**, 9, 3307–3314.

(31) (a) Escartí, F. Complejación con cobre y dopamina de receptores poliaminicos derivados de pirazol. Ph.D. Thesis. Universidad de Valencia, 2008. (b) Garcia-España, E. Unpublished results.

(32) Bringaud, F.; Riviere, L.; Coustou, V. Energy metabolism of trypanosomatids: Adaptation to available carbon sources. *Mol. Biochem. Parasitol.* **2006**, 149 (1), 1–9.

(33) Morales, J.; Mogi, T.; Mineki, S.; Takashima, S.; Mineki, R.; Hirawake, H.; Sakamoto, K.; Omura, S.; Kita, K. Novel mitochondrial complex II isolated from *Trypanosoma cruzi* is composed of 12 peptides including a heterodimeric Ip subunit. *J. Biol. Chem.* **2009**, 284 (11), 7255–7263.

(34) Turrens, J. More differences in energy metabolism between *Trypanosomatidae*. *Parasitol. Today* **1999**, 15 (8), 346–348.

(35) McBride, H.; Neuspiel, M.; Wasiak, S. Mitochondria: More than just a powerhouse. *Curr. Biol.* **2006**, 16, R551–R560.

(36) von Malsburg, K.; Müller, J. M.; Bohnert, M.; Oeljeklaus, S.; Kwiatkowska, P.; Becker, T.; Loniewska-Lwowska, L.; Wiese, S.; Rao, S.; Milenkovic, D.; Hutu, D. P.; Zerbes, R. M.; Schulze-Specking, A.; Meyer, H. E.; Martinou, J. C.; Rospert, S.; Rehling, P.; Meisinger, C.; Veenhuis, M.; Warscheid, B.; van der Klei, I. J.; Pfanner, N.; Chacinska, A.; van der Laan, M. Dual role of mitofilin in mitochondrial membrane organization and protein biogenesis. *Dev. Cell* **2011**, 21, 694–707.

(37) Piacenza, L.; Irigoien, F.; Alvarez, M. N.; Peluffo, G.; Taylor, M. C.; Kelly, J. M.; Wilkinson, S. R.; Radi, R. Mitochondrial superoxide radicals mediate programmed cell death in *Trypanosoma cruzi*: Cytoprotective action of mitochondrial iron superoxide dismutase overexpression. *Biochem. J.* **2007**, 403, 323–334.

(38) Perrin, D. D.; Armarego, W. L. F.; Perrin, D. R. *Purification of Laboratory Chemicals*; Pergamon Press: Oxford, 1980.

(39) Téllez-Meneses, J.; Mejía-Jaramillo, A. M.; Triana-Chávez, O. Biological characterization of *Trypanosoma cruzi* stocks from domestic and sylvatic vectors in Sierra Nevada of Santa Marta, Colombia. *Acta Trop.* **2008**, 108, 26–34.

(40) Osuna, A.; Adroher, F. J.; Lupiáñez, J. A. Influence of electrolytes and non-electrolytes on growth and differentiation of *Trypanosoma cruzi*. *Cell Differ. Dev.* **1990**, 30, 89–95.

(41) Marín, C.; Ramírez-Macías, I.; López-Céspedes, A.; Olmo, F.; Villegas, N.; Díaz, J. G.; Rosales, M. J.; Gutierrez-Sánchez, R.; Sánchez-Moreno, M. In vitro and in vivo trypanocidal activity of flavonoids from *Delphinium staphisagria* against Chagas disease. *J. Nat. Prod.* **2011**, 74, 744–750.

(42) Moreno, D.; Plano, D.; Baquedano, Y.; Jiménez-Ruiz, A.; Palop, J. A.; Sanmartín, C. Antileishmanial activity of imidothiocarbamates and imidoselenocarbamates. *Parasitol. Res.* **2011**, 108, 233–239.

(43) González, P.; Marín, C.; Rodríguez-González, I.; Hitos, A. B.; Rosales, M. J.; Reina, M.; Díaz, J. G.; Gonzalez-Coloma, A.; Sanchez-Moreno, M. In vitro activity of C₂₀-diterpenoid alkaloid derivatives in promastigotes and intracellular amastigotes of *Leishmania infantum*. *Int. J. Antimicrob. Agents* **2005**, 25, 136–141.

(44) Bradford, M. M. A refined and sensitive method for the quantification of microquantities of protein-dye binding. *Anal. Biochem.* **1976**, 72, 248.

(45) Beyer, W. F.; Fridovich, I. Assaying for superoxide dismutase activity: Some large consequences of minor changes in conditions. *Anal. Biochem.* **1987**, 161, 559–566.

(46) Díaz, J. G.; Carmona, A. J.; Perez de Paz, P.; Werner, H. Acylated flavonol glycosides from *Delphinium staphisagria*. *Phytochem. Lett.* **2008**, 1, 125–129.

(47) Longoni, S. S.; Marín, C.; Sauri-Arceo, C. H.; López-Céspedes, A.; Rodríguez-Vivas, R. I.; Villegas, N.; Escobedo-Ortegón, J.; Barrera-Pérez, M. A.; Bolio-Gonzalez, M. E.; Sánchez-Moreno, M. An iron-superoxide dismutase antigen-based serological screening of dogs indicates their potential role in the transmission of cutaneous leishmaniasis and trypanosomiasis in Yucatan, Mexico. *Vector Borne Zoonotic Dis.* **2011**, 11, 815–821.

(48) Fernandez-Becerra, C.; Sánchez-Moreno, M.; Osuna, A.; Opperdoes, F. R. Comparative aspects of energy metabolism in plant trypanosomatids. *J. Eukaryotic Microbiol.* **1997**, 44 (5), 523–529.